Supplemental Material

1. Pre-enrollment screening for biobank participation:

In the initial phase, we will identify all patients referred for a clinical kidney biopsy through electronic health records (EHR). At the kidney biopsy encounter, patients who do not meet any exclusion criteria (under 18 years of age, known pregnancy, additional vulnerable individuals, inability to provide informed consent) are approached for consent in participating in the biorepository (biobank) study, also to provide urine, blood, and kidney tissue samples.

During this process, whole-slide scans of histology, prepared for diagnostic use, are collected. Additionally, a urine sample/pellet (200 cc) is obtained via clean catch, and a blood sample (50 cc) is collected, following the established workflow of the Yale Biobank. The collected samples undergo processing, aliquoting, barcoding, and storage in accordance with the Yale Biobank protocol[S1-4]

1.1 Urine Sample: The samples will be centrifuged at 2000g x 10 minutes to remove cellular debris. Supernatants will be stored in smaller aliquots at -80^{o} C. (https://clinicaltrials.gov /study/NCT04343417)

1.2 Kidney Biopsy [S5]: Prepared biopsy slides will be digitized and scanned at high magnification using the Aperio ScanScope Digital Pathology System provided by the Yale Pathology Digital Imaging services. The slides will be scanned at 40x and will be available for pathologists to establish diagnosis following the workflow of the Biorepository to support research in kidney disease (Yale Biobank).

In order to mitigate potential enrollment losses for the AMP-FSGS trial, among patients referred for biopsy, the biopsy proceduralists, namely Dr. Luciano (Yale Co-I, director of the kidney biopsy service) and Dr. Tokita (MSSM site Co-I), along with their respective research teams, will implement a "flagging" list within EHR. This mechanism will identify patients with a high probability of receiving an FSGS diagnosis based on such as nephrotic syndrome, nephrotic proteinuria, or a urine protein-to-creatinine ratio exceeding 1.5 gm/gm (UPCR > 1.5).

2. Enrollment and randomization:

Patients diagnosed with FSGS and diffuse FPE as indicated in their kidney biopsy report will be approached for the AMP-FSGS. These patients, for whom glucocorticoid therapy for FSGS is planned and alternate diagnoses are excluded, will be approached to consent for the AMP-FSGS trial. (see Table:1 Inclusion and Exclusion criteria). Patients with prior diagnoses of FSGS who are planned for treatment with steroids after a repeat biopsy will also be potential enrollees.

We will utilize a permuted block randomization scheme to ensure blinding and allocation concealment throughout the study. Randomization will be stratified by study site to ensure balance across observed effects of the study drug. The randomization process will be implemented via REDCap. Once consent is signed at either study site, Yale and Mount Sinai, the investigational drug pharmacy services (IDS) will obtain assignment to the appropriate randomization arm and dispense study drug as is appropriate to study limb. The IDS pharmacist will remain unblinded to study limb.

The two study limbs are described as follow:

- **Therapy:** (Prednisone tapered after 3 months (per clinician) + MF (ie Extended release 500 mg daily if eGFR 32-45ml/min, or 1000 mg if eGFR>45 ml/min)

- Control: (Prednisone tapered after 3 months (per clinician) + identical Placebo formulation)

3. Informed consent:

The informed consent will include consent for randomization, sample collection, therapeutic intervention (MF or Placebo). During Visit 9 (Month 5), participants will be approached with a biopsy informed consent form for the purpose of obtaining authorization for a repeat biopsy at 6 months, marking the completion of the study. Importantly, participation in the follow-up biopsy is optional and will not interfere with the overall study participation.

The informed consent documents will be generated in English and Spanish and approved by the single central IRB, and when necessary, consent will be obtained via interpreter services.

4. Intervention:

The overall design and interventions are summarized in Figure 2.

5. Study Visits: The study is organized into 10 visits (summarized details of procedures are outlined in Table 2).

6. Study Assays:

This study aims to investigate the role and mechanisms of MF in FSGS through a pilot randomized trial employing multiparametric assays. The evaluation includes various sample types, such as urine, blood, and kidney biopsy. Both conventional and novel approaches will be applied including serial plasma/urine markers, automated morphometry, podocyte numbers, in-situ proteomics, and single-cell transcriptomics. Additionally, we aim to test the hypothesis that MF improves clinical efficacy outcomes, specifically reducing proteinuria and slowing renal function decline in FSGS. Furthermore, data questionnaire will systematically monitor occurrences of hypoglycemic and gastrointestinal symptoms and concurrently evaluate the overall quality of life.

6.1 Data questionnaire:

6.1.1 Modified KDQOL survey will be used for this study. The modified KDQOL incorporates targeted questions to assess quality of life (QOL).

6.1.2 Gastrointestinal Symptom Rating Scale: In this questionnaire a higher score corresponds to more severe symptoms.

6.1.3 Hypoglycemic symptoms: This questionnaire will evaluate the severity of the symptoms.

All 3 questionnaires have been integrated into the REDCap database and an IPAD will be used for data collection during the study visits.

6.2 Sample Collection and Analysis:

6.2.1 Blood samples: Biomarkers and safety outcomes will be collected and analyzed throughout the study duration. Blood will be collected specifically for the study as well as for standard-of-care labs during the FSGS treatment as required by treating physicians.

Standard-of-care labs: CBC, BMP, hemoglobin A1c, and liver function tests will be collected as part of standard-of-care labs.

Labs to monitor study-related AEs: Plasma lactate, lipid profile, and Vitamin B12 will be collected as part of the research study and will be processed at the clinical laboratory.

Research labs: Plasma and peripheral blood mononuclear cells (PBMC) will be collected as part of the study-specific labs and processed at the central lab.

Blood Sample processing for PBMC and Plasma:

Around 20 ml of blood will be processed at Central Lab. The processing will involve the separation of PBMC, and plasma. Five aliquots of PBMC and three aliquots of plasma will be stored in 2-ml cryovials at liquid nitrogen.

The sample will be processed as mentioned below:

1. Whole blood will be added to a 50 mL centrifuge tube containing 10 mL of sterile PBS.
2. The blood will be gently mixed to achieve the best separation in the next step.
3. Underlay 13 mL of Histopaque (Cat-10771; Sigma Aldrich) into each tube.
4. Centrifuge at 800 g for 30 minutes with the break off.
5. Store the top layer of plasma and pipette off the interphase layer of cells into clean 50 mL centrifuge tubes containing 20 mL of RPMI.
6. Centrifuge this mixture for 7 minutes at 800 g with the break off.
7. Pour off the supernatant liquid and resuspend the cells in 10 mL of RPMI.
8. Add 10ul of trypan blue (Gibco™ 15250061) to 10ul of cells suspension and count the cells using a hemacytometer.
9. After counting cells, centrifuge this mixture for 7 minutes at 800 g with the break off and resuspend the cells in freeze media-I & II to get 5 million cells per vial.

Storage:

Storage of both standard care and research samples, as processed by the local laboratory, will align with the specific guidelines and methodologies established by the local laboratory facilities. The central laboratory will follow the outlined steps for the storage of research samples after processing:

1. Remove centrifuge tubes from the centrifuge machine, pour off the supernatant, and resuspend in the calculated amount of human freeze media-I.
2. Slowly drip the same amount of human freeze media-II into the same tube.
3. Place 1 mL of cell suspension into each cryogenic vial.
4. Pre-freeze a Styrofoam container at -80°C. Place vials into the Styrofoam container in the -80°C freezer overnight.
5. Store the PBMC's in liquid nitrogen for long-term storage.

6.2.2 Urine samples: Both standard of care and research urine samples will facilitate the development of an intra-patient trajectory, enabling comparisons within the trajectory, between study limbs, and with previously published data.

Standard of Care Labs (~5-10ml urine): Standard-of-care assessments will include the collection of urine protein-to-creatinine ratio and 24-hour creatinine clearance. The protein-to-creatinine ratios will be obtained and analyzed on every visit where urine mRNA is processed.

Research Labs (~ 200 ml urine): In the context of research-specific protocols, urine proteomics, urine exosomes (both collected from the urine supernatant), and urine pellet mRNA are integral components of the research laboratories. The Initial focus during the first three post-enrollment visits will be on identifying early changes in urine mRNA (e.g. Nephrin, Podocin), followed by monthly assessments.

The Urine sample processing for mRNA (Fig S1):

The research laboratory will adhere to the following steps in processing the urine samples:

1. Mix well the urine sample using a 25-ml pipette and auto-dispenser. Divide the urine into 50-ml centrifuge tubes by filling maximum of 45-ml urine in each tube.

2. Centrifuge the tubes at 4°C for 25 minutes at 2700 rpm in a swing-out rotor only.

3. Three 15-ml and two 2-ml aliquots of the supernatant will be removed and stored at -80°C and liquid nitrogen respectively for exosomes, biomarker estimation, proteomics, and other measurements.

4. Discard the remaining supernatant and keep the cell pellet on ice flakes. Resuspend the urine cell pellet in 500 µl of cold diethylpyrocarbonate (DEPC)-treated PBS (pH 7.4) by gentle pipetting and transfer the pellet to a new pre-cooled/labeled 1.5 ml centrifuge tubes.

5. Recover the pellet residue at the bottom of the 50-ml centrifuge tube with 500 µl of DEPC-PBS (pH 7.4) and add it to the same 1.5 ml tube.

6. Centrifuge the pellet at 13,000 rpm for 5 minutes at 4°C.

7. Discard the supernatant and resuspend the pellet in 350-500 µl of RLT buffer containing β-mercaptoethanol depending upon pellet size.

8. Freeze the pellet at -80°C for long-term storage.

Urine cell pellet RNA extraction: The total urine pellet RNA was isolated using the RNeasy Mini Kit (# 74106; Qiagen). Urine mRNA concentrations from 10 control samples and 30 biopsy paired samples ranged from 3-160 ng/µl. Reverse transcription is done using high efficiency Superscript-IV (Thermofisher) with increased sensitivity (>/=10pg template cDNA). Quantitation of NPHS2, NPHS1, AQP2, TGFB1, mRNA was done using 7500 Real-Time FAST System (Applied Biosystems) and TaqMan Fast Universal Master Mix, using cDNA in a final volume of 20 µl per reaction. TaqMan Probes (Applied Biosystems) NPHS2 (#Hs00922492_m1), NPHS1 (# Hs00190446_m1), AQP2 (# Hs00166640_m1), and *TGFB1* (#Hs00171257_1ml), were used.

Assay development using SYBR-green: To quantify each gene, we designed qPCR primers recognizing the sequences +/- 150 BP from the midpoint of each TaqMan assay (above). Using expression vectors containing the respective NPHS1, NPHS2, TGFB1, and AQP2 cDNA amplicon sequences, we developed absolute standard curves (10^1 to10^{10} copies per well) with SYBR-green reagent (Fig S1). Next, we generated 10 control samples randomly pooled from 7 healthy volunteers, each of whom donated urine on multiple occasions (~500 ml urine combined in each pooled sample). To establish detection thresholds for each gene in urine samples, qPCR using ~5ng/well of these control cDNA were run to identify optimal dilution points to include in the final standard curve (Applied Biosystems StepOne). These standard dilutions (6 points) are run on every sample plate to generate copy-numbers/µl from every plate. Repeat runs of the same pooled control sample on different plates, as well as the runs of 10 control samples collected at different times from volunteers, provided information into assay variability, and of NPHS2 and NPHS1-mRNA excretion variability in randomly collected samples in homeostasis. Fig S2A shows that nearly all values for these two genes in pooled controls were < 1000 copies per 5ng urinary cDNA. We included 18SRNA (as a measure of total cell RNA) and Uroplakin-1A (as measure of urothelial cells) in the urine pellet to serve as endogenous controls. Neither absorbance ratios of 260/280nm by Nandodrop nor RNA concentrations correlated with mRNA copies of any of the six genes assayed ((Fig S2B & C, respectively), showing limited utility of these metrics in quality control of urine samples.

Assay validation with TaqMan assays: Once standard dilutions were finalized, we utilized the TaqMan assays to confirm detection all six genes in pooled control urine samples. To test the assay in “real world” conditions, we obtained urine samples from a cohort of 30 unselected patients in the Renal division at Yale school of Medicine who were undergoing diagnostic kidney biopsy and enrollment in the Yale nephrology biobank. Table S1 shows clinical epidemiologic details of the biopsy patient cohort. The urine volume in cases ranged from 10-200 ml. Urine processing, cell pellet RNA and qPCR were performed as above using TaqMan assays with 10

control samples on each plate. Two µl of cDNA (5ng/µl) from each urine pellet was run in duplicate. Copy numbers were normalized per ml volume of assayed urine, and/or normalized to urine creatinine concentration (mg/dl). These data (Fig 3) confirmed the detection and quantification of genes of interest in patient collected samples and healthy controls, and demonstrated relatively constant *UPK1A* levels in cases and controls.

Multiplexing: To then develop multiplex assays to optimize RNA use (in case of low yield) and minimize plate-to-plate variation, we combined 3 genes each into two customized multiplex TaqMan assays (one VIC, FAM and NED probe each in each assay; *NPHS2, AQP2, 18SRNA, & NPHS1, UPK1A, TGFB1*). As shown in Fig 3D for NPHS2, RNA quantification from the same urine sample were highly correlated between single-plex and multiplex assays in our biopsy cases/controls ($P<0.001$). For each enrollee in the AMP-FSGS trial, we expect 10 data points for urine cell pellet mRNA with 1 at baseline (before therapy), and one per subsequent visit according to schedule of activities (Table-2). These data will provide trajectory of urine mRNA excretion for each of these genes. Standard curves for each template will be run in every plate will provide copy numbers/µl of each template for direct comparison across plates run at different times. The samples from each visit for patients will be batched during qPCR runs.

6.3 Research Biopsy at 6 months:

***6.3.1 Biopsy procedure*:** The Kidney biopsy procedure will follow the procedures described in the Yale biorepository protocol (https://clinicaltrials.gov/study/NCT04343417) and reported previously[S5].

6.3.2 Informed consent for research biopsy: As noted above, during Visit 9 (Month 5), participants will be provided with a biopsy informed consent form for the purpose of obtaining consent for a repeat biopsy at 6 months, marking the completion of the study. It's important to note that participation in the follow-up biopsy is optional and will not interfere with the overall study participation.

6.3.3 Biopsy sample processing and storage:

The kidney biopsy procedure will adhere to the institution's protocol, involving the collection of three specimens (Formalin for Light Microscopy (LM), Michels solution for Immunofluorescence (IF), and Glutaraldehyde for Electron Microscopy (EM)). Additionally, a portion of the kidney tissue will be preserved in RNAlater solution for processing at the central lab.

The samples processing will follow the Kidney Precision Medicine Project (KPMP) harmonized protocol. The only modification to the standard procedure is that, instead of receiving fresh frozen tissue in a cryomold for immunofluorescence (IF) studies, the IF will be transported for processing in Michel's solution**.**

6.3.4 Paired biopsy assessments: Specimens procured at baseline and 6-months in the subset of patients who consent for repeat research biopsy will be available for paired biopsy assessments.

6.3.4a: Morphometry:

Automated glomerular morphometry: We recently published a deep-learning model[S6, 7] based on both U-Net[S8] and mask R-CNN[S9] algorithms to accurately recognize normal kidney tissue compartments on Aperio-scanned PAS stained images. An adaptation of this algorithm measures glomerular tuft areas (AI-Area) and was validated on PAS images using Weibel-Gomez (W-G) method (n=20). We will utilize the Aperio-scanned images of paired biopsy cohort and apply automated tuft area estimation for all identified glomeruli (see below). Mean AI-Vglom will be calculated from mean AI-Area using W-G equation allowing comparison between case labels. Globally sclerosed glomeruli are excluded.

Non-glomerular parameters: Glomerular numerical- and area-density (per unit cortical area to estimate nephron endowment), percentage of area with interstitial fibrosis and/or atrophic tubules, and area of interstitial infiltrates are all simultaneously evaluated by our AI-algorithm[S6] in all scanned images.

Analysis: Unbiased comparison of these AI-developed parameters will be done in paired-biopsy cohort using (i) final biopsies between therapy limbs (MF vs Placebo), and (ii) between initial and final biopsy within the MF therapy limb, to identify restriction of glomerulomegaly in FSGS by MF. (iii) In addition, individual AI-developed parameters, and composite AI-scores (ITAS and CDS) will be applied to *all enrollee biopsies* (n=30) and correlated with clinical and mechanistic prognostic indicators (see Podocinuria section).

6.3.4b. Single nuclear transcriptomics:

Single nuclear RNAseq will be performed on the extra biopsy core (which is immediately stored in RNA-later), specifically in the subset of enrollees in the trial who consent for repeat biopsy (expected N for single nuclear data~10). *Single nuclear preparation* from samples stored in RNA-later will be per Kidney Precision medicine project as described[S10, 11] i.e. sample cutting (<2mm), douncer homogenization, chilled Nuclei EZ buffer lysis, 70- to 5-mcM filtration, and library generation. Single nuclei are resuspended in the PN-2000153 buffer and loaded 10000 nuclei/lane per the 10X genomics protocol.

Analyses: Our summarized analysis pipeline for this subaim is in FigS3: Integration and unsupervised clustering of data will be performed using Seurat, and each glomerular cell type will be annotated with canonical markers (50K reads/cell). Within each cell type, DEGs will be identified using FindMarker (Seurat package) in the following comparisons (a) within-patient *and* within-group between paired biopsies, and (b) between the two treatment groups in repeat biopsies. KEGG and GO enrichment analysis of DEGs, kinase enrichment assay will be performed with ClusterProfiler for unbiased analyses, and for AMPK-activation[S12].The identified podocyte-specific DEGs in (a) and (b) will be compared with the following. **(i) *MCD enriched DEGs:*** Currently, NEPTUNE has additional glomerular transcriptomes obtained from RNA-seq of micro-dissected NS biopsies**.** We are currently expanding our preliminary data by comparing DEGs between all MCD and FSGS case labels using these RNA-seq data (serving as independent and technical validation). Briefly, DEGs will be identified from each comparison,

using LIMMA test at FDR =5% and enriched pathways or GO functional terms will be determined by Fisher-exact test with p value of 0.05. *Covariates:* Analyses will be adjusted by gender, age, adult vs pediatric status to identify unique DEGS. *Podocyte-expressed DEGs* will then be identified in these analysis using the pipelines described before[S13, 14]. **(ii) *Cross-species analyses for AMPK-regulated and specific DEGS:*** Here, the DEGs enriched in podocytes in MF-treated biopsies will be compared to single cell transcriptome data from AMPK-activation animals vs controls (n=5 animals per condition; 150-BP, ~10-million paired-end reads, per animal). For this, we crossed AMPK-activation mice (γ1D316A-transgenic with active γ-subunit; Gift from Dr David Carling, London) into podocyte specific expression(Nphs1-cre) to generate a unique *podocyte specific AMPK-activation model*. Podocyte lysates from adult PRKAGm-mice confirmed enhanced AMPK-activation, and showed reduced glomerular, podocyte- and capillary + endothelial - volumes vs littermate controls, consistent with findings from pharmacologic AMPK-modulation. Podocyte- enriched DEGs from single nuclear data of this murine model of podocyte specific AMPK-activation (being generated as part of an NIDDK funded animal study), will be evaluated using cross-species transcriptional network comparisons, to identify overlapping DEGs of AMPK enrichment with MF. (iii) *Evaluation of non podocyte **kidney cells:*** MF-treated non-podocyte-nuclear transcriptomes (glomerular-, tubular- and infiltrating cells) between MF and control limbs, or between baseline and 6m MF-biopsies, will also each be evaluated for enrichment of AMPK signaling within each cell-type. *Enrichment:* Single cell enrichment analysis of DEGs will be performed with ClusterProfiler for unbiased analyses[S12]. In bulk and single cell analyses, from significant DEGs (gene lists shown in Fig S3), enriched pathway terms (KEGG, GO function terms, kinase enrichment assay etc.), and upstream regulatory elements (Transfac/Jaspar, etc.) will be identified, and mapped using established comparison pipe-lines[S15, 16], with a goal to discover candidates for IMC.

6.3.4c Imaging Mass cytometry:

IMC panel development: We have developed a customized IMC panel of heavy metal-conjugated antibodies combining candidates from prior work [S17, 18] for (a) major cell types in glomeruli (WT1/Nestin/Vimentin: podocytes, SMA: Mesangeal cells, b-catenin: Parietal epithelium, ERG/CD31:endothelia), in tubules (Megalin:PCT, THP:Thick ascending limb, Calbindin:DCT, AQP2 :collecting duct), in inflammatory infiltrates (6 markers), and in stroma (SMA, COL4), with (b) novel Ampk-related signals (LC3b, p62, p-Tyrosine, p-AMPK^{U}, FYN^{U})[^{U}= requiring validation]) and (c) injury/repair markers (KIM1/Ki67). DNA intercalators (193Ir) will identify nuclei. *Imaging:* For all probed images, identical signal thresholding to remove background, and setting of signal intensity range (0 to 100) will be performed for each marker allowing quantitative comparison between samples[S17]. Using our Kidney-MAPPS pipeline, a nearest-neighbor–based clustering approach using intensity readouts of whole slide-images for individual cell-type markers enables assignment of cell-type based on intensity profile (as described in[S17, 18]).

Targeted analyses: The following groups will be examined to evaluate AMPK-activation by MF (i) final biopsies between therapy limbs (MF vs Placebo), and (ii) initial- and final- biopsies within-patient, and within the MF therapy limb. In labelled podocytes (WT1/Nestin co-labelled cells), intensity values of pAMPK, p62, Fyn, p-Tyrosine, LC3, and intensity correlations P-Tyrosine: FYN, LC3B:Nestin will be compared using -per podocyte, -per glomerulus and -per biopsy analyses.

Podocyte counting between initial and final biopsies will be performed in paired samples using WT1 Immunofluorescence and using IMC readouts. Podocyte counts will be correlated with podocyturia.

Supervised analyses: FSGS cases will be clustered using initial biopsies and correlating to prognostic features i.e. with podocyturia (and mechanistic) and/or clinical outcomes. Here intensities of all evaluated markers will be compared in a case control manner using Linear models

for microarray (Bioconductor LIMMA for R) and FDR-adjusted P-values of 0.05 will be considered significant. *Unsupervised cluster analyses* will also be applied for subset discovery.

Sample size: We will apply IMC to the paired biopsy cohort of 10 FSGS enrollees.

Sample size for IF (technical validation): Optimal markers (up to 3) identified by IMC will be evaluated using immunofluorescence in institutional biorepositories to confirm differential signals between MCD and FSGS, and evaluate association with outcomes.

7. Statistical Plan and Data Analyses:

7.1 Database: Data will be collected prospectively as described above. All data will be entered in duplicate by trained study coordinators using a secure, HIPAA-compliant cloud-based platform (REDCap). Disagreement in data entry will be resolved by direct discussion among study coordinators, with the PI being ultimately responsible for data classification and accuracy.

7.2 Blinding procedure: The study team will remain blinded to intervention status throughout the study, and only the investigational drug pharmacy will have access to the centralized randomization module. Allocation concealment will be maintained as the computerized tool requires documented consent before randomization can occur (thereby not allowing bias in the consent process) and by including a permuted-block randomization structure which makes prediction of subsequent randomization status nearly impossible.

7.3 Randomization: We will use a block-randomization scheme using permuted blocks of length 4-, 6-, and 8 individuals. Randomization will be stratified by study site.

7.4 Unblinding: Data will only be unblinded when all primary study outcome data has been collected, or if requested by the DSMB or other regulatory bodies.

7.5 Baseline data: We will examine summary statistics of participants using counts, proportions, measures of central tendency and dispersion as appropriate. All analyses will be based on the intention to treat principle such that individuals randomized to MF will be analyzed together, regardless of receipt or adherence to the MF regimen. We also plan to perform per-protocol

analyses at the end of the study. The per-protocol dataset will include all participants who demonstrate >=75% adherence to the study drug (as assessed via pill counts at study visits) and complete the final study visit

7.6 Outcomes: We will compare categorical clinical outcomes (such as remission rates) between the treatment groups using the Fisher exact test or chi-square test based on data sparsity, and continuous outcomes using the Wilcoxon rank-sum test.

Within-individual change outcomes: We will use mixed-effects models, including a time-interaction term to evaluate slope outcomes, such as change of proteinuria and eGFR, change in biomarker levels, and change in Log podocinuria in the urine across the two groups. We will explore various covariance structures and the use of random intercepts / slopes based on model fit as assessed by the Akaike information criterion (AIC).

Mechanistic outcomes: As this is a pilot study of a relatively rare condition, we are maximizing the possibility of discovering important mechanistic insights through relatively broad biomarker characterization, using both hypothesis-driven (Mesoscale) and less biased (O-Link) approaches. We recognize that, in the face of multiple analyses, the false discovery rate increases. Although we will use a p-value of 0.05 as a marker of statistical significance, we will be cautious in our interpretation of statistically significant findings, treating them as potential targets for further study in a larger-scale trial. Additionally, we will engage in several dimensionality reduction techniques to minimize the dataspace being evaluated. This will include principal component analysis[S19], consensus-based-clustering[S20], and Potential of Heat-diffusion for Affinity-Based Transition Embedding (PHATE) analysis[S21]. These approaches may reveal underlying data structures and provide mechanistic insights that are robust to the large number of individual analytes being measured.

7.7 Safety outcomes: Rare safety events may not rise to the level of statistical significance in a pilot trial of this type. As such, while we will calculate measures of association between treatment and safety events, we will present the data in aggregate to the DSMB as per our study monitoring

plan. We will instruct the DMSB to consider that safety concerns do not need to rest on a statistically significant p-value framework to nevertheless be important and addressable.

QOL assessment: In the patient data questionnaire, we will score the KD-QOL survey based on previously-published criteria, which includes a composite score as well as five sub-scales: Physical function, mental function, burden of kidney disease, symptoms, and effect of kidney disease on daily life. The GSRS responses will be scored with a composite score and 14-subscores (ranging from 0-to-6, for no symptoms-to-severe symptoms). We will examine scores across these domains at baseline, monthly, at 6-months and utilize mixed-effects models with a treatment interaction term to determine if there is a significant impact of treatment on various QOL domains and GSRS components.

7.8 Sample size and Power Analyses: While the purpose of our pilot trial is to generate estimates of outcome rates to inform the design of a larger trial, we calculate that by enrolling 30 individuals (15 in each treatment group), we will have 80% power to detect at least a 1.1 standard deviation difference in continuous outcomes. Our preliminary murine data from using AMPK-activation strategies i.e. Metformin (MF), PF0640957 (PF) or Shroom3-knockdown published in JCI-insight (Ref 7 in the manuscript) suggested that differences in levels of creatinine (~20-45% reduction), BUN (~30-50% reduction), AMPK activation (>200% increase in phospho-AMPK), glomerular volume (~15-33% reduction), podocyte counts by WT1 stain (~20% improvement) and albumin-creatinine ratio (6-10 fold reduction) using AMPK activators in multiple FSGS models exceeded this threshold.

Yale performed 222 biopsies in the last 2 years with 38 having FSGS. With Mount Sinai (150 biopsies per year; Co-I: Dr He), we anticipate no difficulty reaching our recruitment goal, but will expand the study to other medical centers (Johns Hopkins University under Dr Chirag Parikh– where we have established MTAs for biobank sample transfer and track record of clinical trial collaboration), should recruitment prove more difficult than expected. Additionally, based on

enrollment rate in Months 3-18, we will consider enrolling individuals who are not explicitly planned for steroid therapy provided there is a clinical suspicion that the etiology is primary FSGS. In this eventuality, we will stratify randomization to ensure those not receiving steroids are equally balanced between treatment arms.

7.9 Statistical software: All statistical analyses will be performed in GraphPad prism, R, Python, Stata, and SAS.

Supplemental References

S1. Moledina DG, Obeid W, Smith RN, et al. Identification and validation of urinary CXCL9 as a biomarker for diagnosis of acute interstitial nephritis. *J Clin Invest* 2023; **133**: e168950.

S2. Qian L, Menez S, Hu D, et al. Safety and Adequacy of Kidney Biopsy Procedure in Patients with Obesity. *Kidney360* 2023; **4**: 98-101.

S3. Melchinger H, Calderon-Gutierrez F, Obeid W, et al. Urine Uromodulin as a Biomarker of Kidney Tubulointerstitial Fibrosis. *Clin J Am Soc Nephrol* 2022; **17**: 1284-1292.

S4. Moledina DG, Wilson FP, Kukova L, et al. Urine interleukin-9 and tumor necrosis factor-alpha for prognosis of human acute interstitial nephritis. *Nephrol Dial Transplant* 2021; **36**: 1851-1858.

S5. Moledina DG, Cheung B, Kukova L, et al. A Survey of Patient Attitudes Toward Participation in Biopsy-Based Kidney Research. *Kidney Int Rep* 2018; **3**: 412-416.

S6. Zhengzi Yi FS, Madhav C Menon, Karen Keung, Caixia Xi, Sebastian Hultin, M. Rizwan Haroon Al Rasheed, Li Li, Fei Su, Zeguo Sun, Chengguo Wei, Weiqing Huang, Samuel Fredericks, Qisheng Lin, Khadija Banu, Germaine Wong, Natasha M. Rogers, Samira Farouk, Paolo Cravedi, Meena Shingde, R. Neal Smith, Ivy A. Rosales, Philip J. O'Connell, Robert B. Colvin, Barbara Murphy, Weijia Zhang: Deep learning identifies pathological abnormalities predictive of graft loss in kidney transplant biopsies. *biorxiv, Cold Spring harbor*, 2021, **101**: 288-298

S7. Yi Z, Salem F, Menon MC, et al. Deep learning identified pathological abnormalities predictive of graft loss in kidney transplant biopsies. *Kidney Int* 2022; **101**: 288-298.

S8. Jayapandian CP, Chen Y, Janowczyk AR, et al. Development and evaluation of deep learning-based segmentation of histologic structures in the kidney cortex with multiple histologic stains. *Kidney Int* 2021; **99**: 86-101.

S9. Wang Y, Liu X, Wang W, et al. Long-term Clinical Outcomes of US-Guided High-Intensity Focused Ultrasound Ablation for Symptomatic Submucosal Fibroids: A Retrospective Comparison with Uterus-Sparing Surgery. *Acad Radiol* 2020 **28**:1102-1107.

S10. Menon R, Bomback AS, Lake BB, et al. Integrated single-cell sequencing and histopathological analyses reveal diverse injury and repair responses in a participant with acute kidney injury: a clinical-molecular-pathologic correlation. *Kidney Int* 2022; **101**:1116-1125.

S11. Lake BB, Menon R, Winfree S, et al. An atlas of healthy and injured cell states and niches in the human kidney. *Nature 2023*; **619**: 585-594.

S12. Zhang Z, Sun Z, Fu J, et al. Recipient APOL1 risk alleles associate with death-censored renal allograft survival and rejection episodes. *J Clin Invest* 2021; **131**: e146643.

S13. Fu J, Wei C, Lee K, et al. Comparison of Glomerular and Podocyte mRNA Profiles in Streptozotocin-Induced Diabetes. *J Am Soc Nephrol* 2016; **27**: 1006-1014.

S14. Wei C, Banu K, Garzon F, et al. SHROOM3-FYN Interaction Regulates Nephrin Phosphorylation and Affects Albuminuria in Allografts. *J Am Soc Nephrol* 2018; **29**: 2641-2657.

S15. Hodgin JB, Nair V, Zhang H, et al. Identification of cross-species shared transcriptional networks of diabetic nephropathy in human and mouse glomeruli. *Diabetes* 2013; **62**: 299-308.

S16. Berthier CC, Bethunaickan R, Gonzalez-Rivera T, et al. Cross-species transcriptional network analysis defines shared inflammatory responses in murine and human lupus nephritis. *J Immunol* 2012; **189**: 988-1001.

S17. Singh N, Avigan ZM, Kliegel JA, et al. Development of a 2-dimensional atlas of the human kidney with imaging mass cytometry. *JCI Insight* 2019; **4** e129477.

S18. Avigan ZM, Singh N, Kliegel JA, et al. Tubular Cell Dropout in Preimplantation Deceased Donor Biopsies as a Predictor of Delayed Graft Function. *Transplant Direct* 2021; **7**: e716.

S19. O'Connell PJ, Zhang W, Menon MC, et al. Biopsy transcriptome expression profiling to identify kidney transplants at risk of chronic injury: a multicentre, prospective study. *Lancet* 2016; **388**: 983-993.

S20. Lancichinetti A, Fortunato S. Consensus clustering in complex networks. *Sci Rep* 2012; **2**: 336.

S21. Moon KR, van Dijk D, Wang Z, et al. Visualizing structure and transitions in high-dimensional biological data. *Nature biotechnology* 2019; **37**: 1482-1492.

Supplemental Figures

Fig S1:

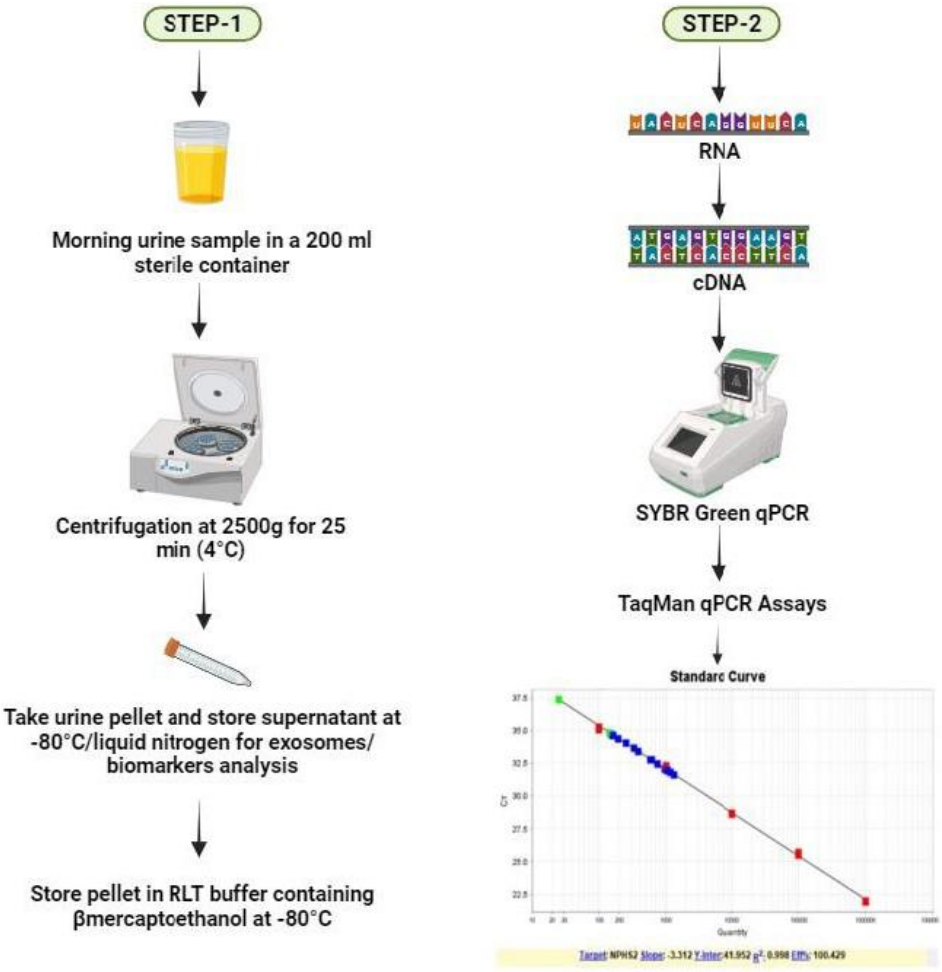

Figure S1: Urine processing and pellet QPCR: Step-1: Flowchart showing harmonized urine processing steps starting with urine collection in a sterile, sealed container, followed by centrifugation for cell pellet and storage in RLT-buffer. Step-2: At a later date, total urine pellet RNA is extracted using the RNeasy Mini Kit, and reverse transcription is performed. Initial detection and quantification of urinary mRNA was established using SYBR-green reagents and in-house primers. Absolute standard curves were generated using expression plasmids for each gene. Urinary mRNA detection/ quantification assays were finalized using customized TaqMan assays (Suppl methods). The standard curve shown in step 2 represents R2=0.998 and efficiency of 100.24% to detect NPHS2 copies. Red dots shows five standards while blue/green dots represent test samples run in this plate.

Fig S2:

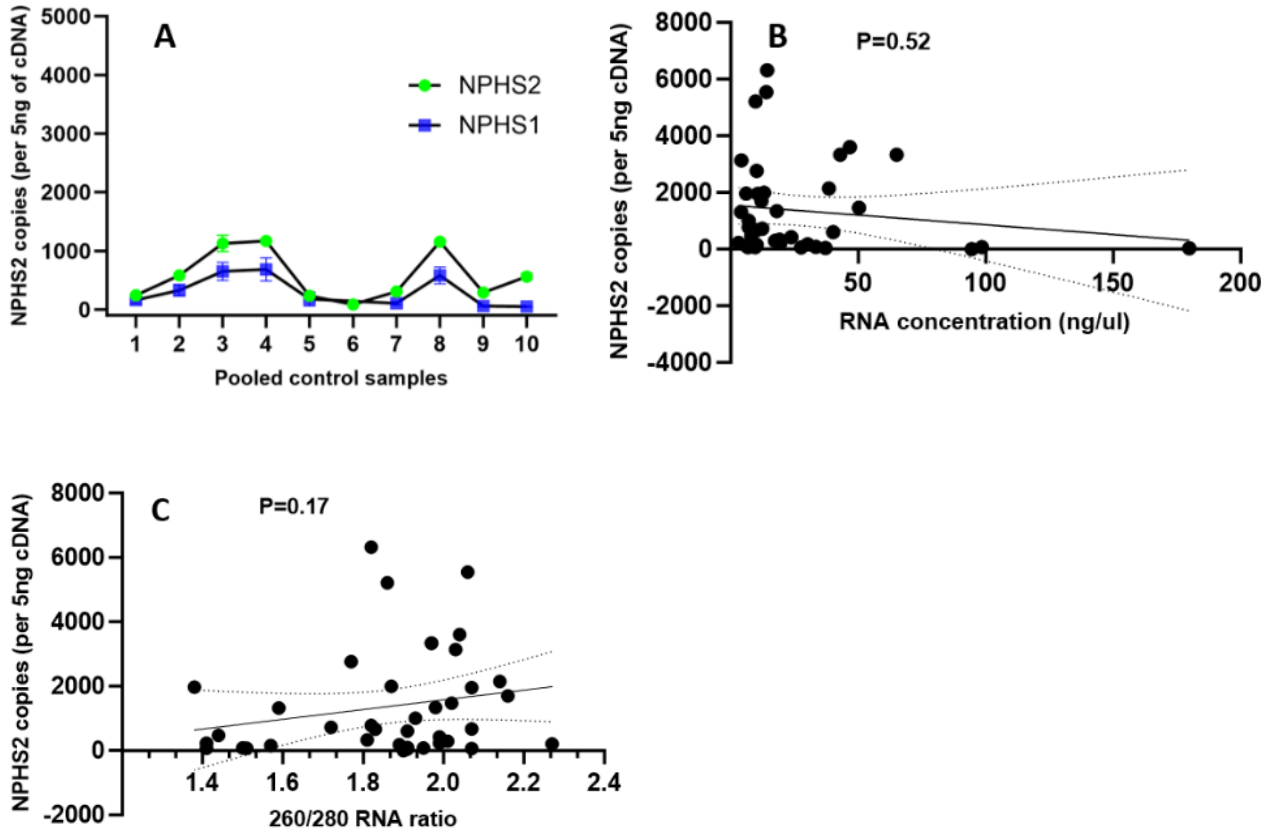

Figure S2: Quality control metrics of Urine pellet mRNA. (A) Line diagrams show the mean/standard error of NPHS2- (green dots with error bars) and NPHS1- (Blue dots with error bars) shows copies/5ng cDNA of 10 pooled control urine samples to provide an estimate of variability of these urine mRNAs. Individual samples obtained at different times from 7 healthy controls were variably pooled to generate ~500 ml urine/pooled sample. Pooled samples were utilized to obtain larger cell pellets in each control to allow multiple runs of the same sample across plates. (B-C) Correlation plot of Urine NPHS2 with (B) RNA concentration [range 3-160 ng/mcl] and (C) with 260/280 ratio [range 1.38-2.27] by nanodrop (n=40), showing absence of significant correlations. Similar evaluation of NPHS1, UPK1A, TGFB1, AQP2 & 18SRNA showed no significant correlations of copy numbers with these quality metrics (not shown).

Fig S3:

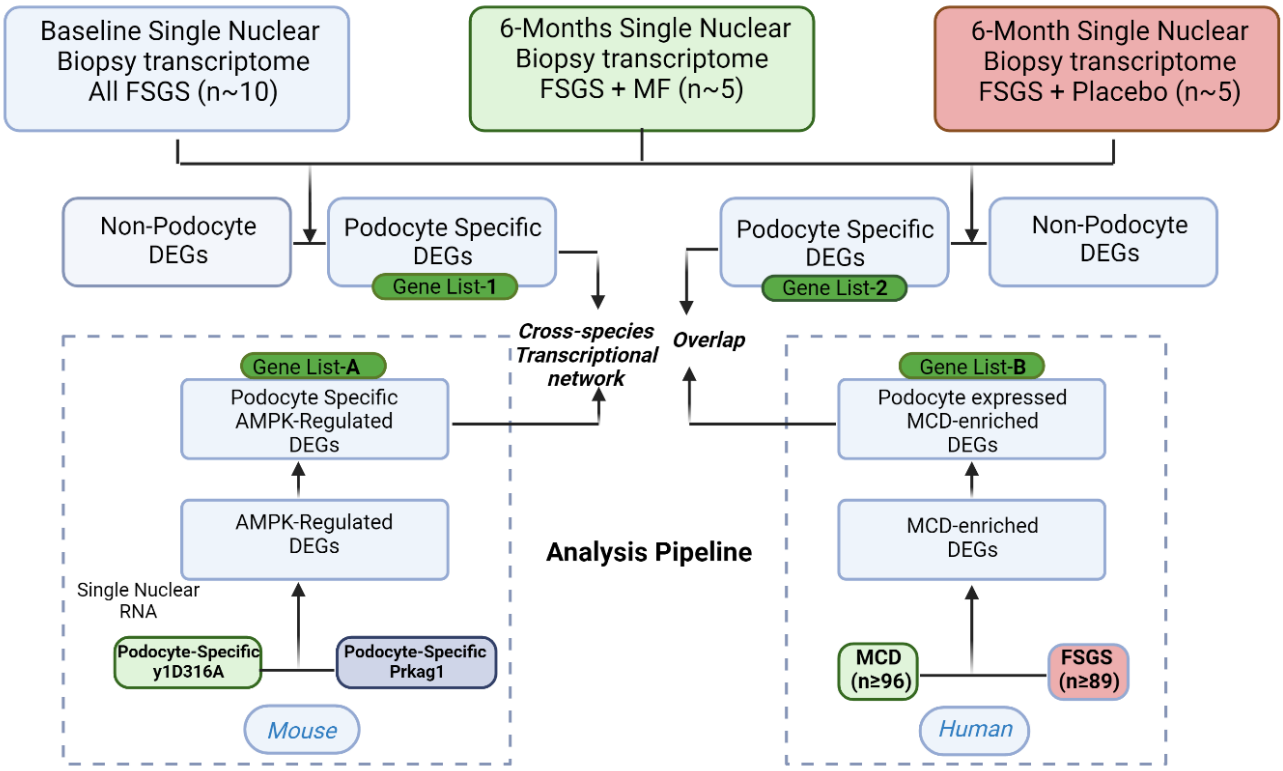

Figure S3: Transcriptome analyses pipeline for biopsy single nuclear RNAseq: Schematic describes transcriptome analysis pipeline of single nuclear transcriptomes from subset of patients with paired kidney biopsies. Our goals are to evaluate (a) AMPK activation in podocytes with MF treatment using a podocyte-specific AMPK-activation mouse model (b) evaluate DEGs between known MCD vs FSGS comparisons from the NEPTUNE cohort with MF- vs placebo treatment (c) identify consistently dysregulated genes (>2 fold) that could be tested at the protein level in biopsies (d) identify putative ligand-receptor interactions using our generated proteomic data.

Table-S1: DEMOGRAPHIC OF CASES AND BIOPSY CONTROLS

	Cases (N=30)	Controls (N=7)
Age		
Mean	55.7 ± 16.09	34.1 ± 7.07
Median	58.5	34
Self reported Race		
White	21 (70%)	3 (42.8%)
Black	4 (13.33%)	0 (0%)
Asian	1 (3.33%)	4 (57%%)
Unknown	4 (13.33%)	0 (0%)
Gender		
Male	18 (60%)	7 (100%)
Female	12 (40%)	0 (0%)
Dipstick leukocytes		
Negative	21 (70%)	NA
+	7 (23.33%)	
+++	2 (6.66%)	
Primary biopsy diagnosis		
Diabetic kidney disease	4 (13.3%)	NA
Acute tubular necrosis	13 (43.3%)	
FSGS	3 (10%)	
Others	2 (6.6%)	
Glomerulonephritis	8 (26.7%)	
Renal Function		
Creatinine	1.91 ± 0.96	NA
eGFR	47.22 ± 27.71	
Protein:Creatinine ratio (g/g)	2.32 ± 2.54	NA

eGFR- Estimated glomerular filtration rate, FSGS- Focal segmental glomerulosclerosis, N- number of patients, NA- not available.

1. Moledina DG, Obeid W, Smith RN*, et al.* Identification and validation of urinary CXCL9 as a biomarker for diagnosis of acute interstitial nephritis. *J Clin Invest* 2023; **133**.

2. Qian L, Menez S, Hu D*, et al.* Safety and Adequacy of Kidney Biopsy Procedure in Patients with Obesity. *Kidney360* 2023; **4:** 98-101.

3. Melchinger H, Calderon-Gutierrez F, Obeid W*, et al.* Urine Uromodulin as a Biomarker of Kidney Tubulointerstitial Fibrosis. *Clin J Am Soc Nephrol* 2022; **17:** 1284-1292.

4. Moledina DG, Wilson FP, Kukova L*, et al.* Urine interleukin-9 and tumor necrosis factor-alpha for prognosis of human acute interstitial nephritis. *Nephrol Dial Transplant* 2021; **36:** 1851-1858.

5. Moledina DG, Cheung B, Kukova L*, et al.* A Survey of Patient Attitudes Toward Participation in Biopsy-Based Kidney Research. *Kidney Int Rep* 2018; **3:** 412-416.

6. Zhengzi Yi FS, Madhav C Menon, Karen Keung, Caixia Xi, Sebastian Hultin, M. Rizwan Haroon Al Rasheed, Li Li, Fei Su, Zeguo Sun, Chengguo Wei, Weiqing Huang, Samuel Fredericks, Qisheng Lin, Khadija Banu, Germaine Wong, Natasha M. Rogers, Samira Farouk, Paolo Cravedi, Meena Shingde, R. Neal Smith, Ivy A. Rosales, Philip J. O'Connell, Robert B. Colvin, Barbara Murphy, Weijia Zhang: Deep learning identifies pathological abnormalities predictive of graft loss in kidney transplant biopsies. In (vol 2021), biorxiv, Cold Spring harbor, 2021

7. Yi Z, Salem F, Menon MC*, et al.* Deep learning identified pathological abnormalities predictive of graft loss in kidney transplant biopsies. *Kidney Int* 2022; **101:** 288-298.

8. Jayapandian CP, Chen Y, Janowczyk AR*, et al.* Development and evaluation of deep learning-based segmentation of histologic structures in the kidney cortex with multiple histologic stains. *Kidney Int* 2021; **99:** 86-101.

9. Wang Y, Liu X, Wang W*, et al.* Long-term Clinical Outcomes of US-Guided High-Intensity Focused Ultrasound Ablation for Symptomatic Submucosal Fibroids: A Retrospective Comparison with Uterus-Sparing Surgery. *Acad Radiol* 2020.

10. Menon R, Bomback AS, Lake BB*, et al.* Integrated single-cell sequencing and histopathological analyses reveal diverse injury and repair responses in a participant with acute kidney injury: a clinical-molecular-pathologic correlation. *Kidney Int* 2022.

11. Lake BB, Menon R, Winfree S*, et al.* An atlas of healthy and injured cell states and niches in the human kidney. *Nature* 2023; **619:** 585-594.

12. Zhang Z, Sun Z, Fu J*, et al.* Recipient APOL1 risk alleles associate with death-censored renal allograft survival and rejection episodes. *J Clin Invest* 2021; **131**.

13. Fu J, Wei C, Lee K*, et al.* Comparison of Glomerular and Podocyte mRNA Profiles in Streptozotocin-Induced Diabetes. *J Am Soc Nephrol* 2016; **27:** 1006-1014.

14. Wei C, Banu K, Garzon F*, et al.* SHROOM3-FYN Interaction Regulates Nephrin Phosphorylation and Affects Albuminuria in Allografts. *J Am Soc Nephrol* 2018; **29:** 2641-2657.

15. Hodgin JB, Nair V, Zhang H*, et al.* Identification of cross-species shared transcriptional networks of diabetic nephropathy in human and mouse glomeruli. *Diabetes* 2013; **62:** 299-308.

16. Berthier CC, Bethunaickan R, Gonzalez-Rivera T*, et al.* Cross-species transcriptional network analysis defines shared inflammatory responses in murine and human lupus nephritis. *J Immunol* 2012; **189:** 988-1001.

17. Singh N, Avigan ZM, Kliegel JA*, et al.* Development of a 2-dimensional atlas of the human kidney with imaging mass cytometry. *JCI Insight* 2019; **4**.

18. Avigan ZM, Singh N, Kliegel JA*, et al.* Tubular Cell Dropout in Preimplantation Deceased Donor Biopsies as a Predictor of Delayed Graft Function. *Transplant Direct* 2021; **7:** e716.

19. O'Connell PJ, Zhang W, Menon MC*, et al.* Biopsy transcriptome expression profiling to identify kidney transplants at risk of chronic injury: a multicentre, prospective study. *Lancet* 2016; **388:** 983-993.

20. Lancichinetti A, Fortunato S. Consensus clustering in complex networks. *Sci Rep* 2012; **2:** 336.

21. Kevin R. Moon DvD, Zheng Wang, Daniel Burkhardt, William S. Chen, Antonia van den Elzen, Matthew J. Hirn, Ronald R. Coifman, Natalia B. Ivanova, Guy Wolf, Smita Krishnaswamy: Visualizing Transitions and Structure for High Dimensional Data Exploration. In (vol 2022), BioRxiv, Cold Spring Harbor Laboratory, 2017, p High dimensional data visualization